

Enhancing the organic solvent resistance of transaminase from *Aspergillus terreus* by regional random mutation

Chun-Ning Wang¹, Shuai Qiu¹, Fang-Fang Fan¹, Chang-Jiang Lyu¹, Sheng Hu¹, Wei-Rui Zhao¹, Jia-Qi Mei¹, Le-He Mei¹, and Jun Huang¹

¹Affiliation not available

March 14, 2023

Abstract

Biocatalysis in high-concentration organic solvents has been applied to produce various industrial products with many advantages. However, using enzymes in organic solvents often suffers from inactivation or decreased catalytic activity and stability. So, improving the tolerance of enzymes in organic solvents is essential. Herein, the method of regional random mutation combined with combinatorial mutation was used to improve the resistance of transaminase from *Aspergillus terreus* (AtATA) in organic solvents, and the best mutant T23I/T200K/P260S (M3) was acquired. In different concentrations of dimethyl sulfoxide (DMSO), the catalytic efficiency toward 1-acetylnaphthalene and the stability were higher than the wild-type (WT) of AtATA. M3 also showed enhanced stability against six organic solvents with different oil-water partition coefficients (log P values). The results of decreased Root Mean Square Fluctuation (RMSF) values via 20-ns molecular dynamics simulations under different concentration DMSO revealed that mutant M3 had lower flexibility, acquiring a more stable protein structure and contributing to its organic solvents stability than WT. Intra- and intermolecular interaction analysis indicated that the increased hydrogen bonds and hydrophobic interactions within monomers or at the interface of two monomers also strengthened the stability of the overall structure against organic solvents. Furthermore, M3 was applied to convert 1-acetylnaphthalene for synthesizing (R)-(+)-1(1-naphthyl)-ethylamine ((R)-NEA), which was an intermediate of Cinacalcet Hydrochloride. Moreover, 3~10 mM 1-acetylnaphthalene can be converted to (R)-NEA with 94.2~38.9% yield and a strict R-stereoselectivity within 10 h under 25% DMSO, which was higher than WT and expected to be a potential biocatalyst for industrial application.

Enhancing the organic solvent resistance of transaminase from *Aspergillus terreus* by regional random mutation

Chun-Ning Wang¹, Shuai Qiu^{1*}, Fang-Fang Fan¹, Chang-Jiang Lyu¹, Sheng Hu², Wei-Rui Zhao², Jia-Qi Mei³, Le-He Mei^{2,4,5*}, Jun Huang^{1*}

¹Key Laboratory of Chemical and Biological Processing Technology for Farm Products of Zhejiang Province, Zhejiang Provincial Collaborative Innovation Center of Agricultural Biological Resources Biochemical Manufacturing, School of Biological and Chemical Engineering, Zhejiang University of Science and Technology, Hangzhou 310023, China

²School of Biological and Chemical Engineering, Ningbo Tech University, Ningbo, 315100, China ³Hangzhou Huadong Medicine Group Co. Ltd, Hangzhou 310011, China

⁴College of Chemical and Biological Engineering, Zhejiang University, Hangzhou, 310027, China

⁵Jinhua Advanced Research Institute, Jinhua, 321019, China

*Corresponding author: Prof. Jun Huang, Dr. Shuai Qiu, Prof. Le-He Mei

Email: huangjun@zust.edu.cn (Jun Huang), qiushuai@zust.edu.cn (Shuai Qiu), meilh@zju.edu.cn (Le-He Mei)

Tel.: +86-571-85070369; Fax: +86-571-85070369

Abstract

Background: Biocatalysis in high-concentration organic solvents has been applied to produce various industrial products with many advantages. However, using enzymes in organic solvents often suffers from inactivation or decreased catalytic activity and stability. So, improving the tolerance of enzymes in organic solvents is essential.

Main methods and results: Herein, the method of regional random mutation combined with combinatorial mutation was used to improve the resistance of transaminase from *Aspergillus terreus* (*At* ATA) in organic solvents, and the best mutant T23I/T200K/P260S (M3) was acquired. In different concentrations (ranging from 25% to 45%, *v/v*) of dimethyl sulfoxide (DMSO), the catalytic efficiency ($k_{\text{cat}}/K_{\text{m}}$) toward 1-acetylnaphthalene and the stability (half-life $t_{1/2}$) were higher than the wild-type (WT) of *At* ATA. M3 also showed enhanced stability against six organic solvents with different oil-water partition coefficients (log *P* values). The results of decreased Root Mean Square Fluctuation (RMSF) values via 20-ns molecular dynamics (MD) simulations under 15%, 25%, 35%, and 45% DMSO revealed that mutant M3 had lower flexibility, acquiring a more stable protein structure and contributing to its organic solvents stability than WT. Intra- and intermolecular interaction analysis indicated that the increased hydrogen bonds and hydrophobic interactions within monomers or at the interface of two monomers also strengthened the stability of the overall structure against organic solvents. Furthermore, M3 was applied to convert 1-acetylnaphthalene for synthesizing (*R*)-(+)-1-(1-naphthyl)-ethylamine ((*R*)-NEA), which was a resolving agent for producing L-menthol by resolution of monomenthyl phthalate, and an intermediate of Cinacalcet Hydrochloride for the treatment of secondary hyperthyroidism and hypercalcemia. Moreover, 3~10 mM 1-acetylnaphthalene can be converted to (*R*)-NEA with 94.2~38.9% yield and a strict *R*-stereoselectivity (enantiomeric excess (*e.e.*) value >99.5%) within 10 h under 25% DMSO, which was higher than WT and expected to be a potential biocatalyst for industrial application.

Conclusion: The beneficial mutation sites were identified to tailor *At* ATA's organic solvents stability via regional random mutation. The "best" mutant T23I/T200K/P260S (M3) holds great potential application for the synthesis of (*R*)-NEA.

Keywords: transaminase, organic solvent stability, regional random mutation, MD simulations, (*R*)-(+)-1-(1-naphthyl)-ethylamine

1. Introduction

(*R*)-1-(1-Naphthyl)-ethylamine ((*R*)-NEA) is a critical chiral aromatic amine compound, which is widely used in pharmaceutical industry, chemical industry, materials and other fields.^[1] For example, (*R*)-NEA can be used as a resolving agent for acid/ester enantiomers by exploiting the weakly basic chemical properties of amino group.^[2] Dudas et al. reported (*R*)-NEA was a resolving agent for producing L-menthol by resolution of monomenthyl phthalate.^[2] Moreover, (*R*)-NEA can be used to prepare the intermediate of Cinacalcet Hydrochloride from 1-acetylnaphthalene, which is a kind of pharmaceutical for the treatment of secondary hyperthyroidism and hypercalcemia.^[3] The synthesis of (*R*)-NEA via biocatalysts, such as amine oxidases, imine reductase, amine dehydrogenases, and transaminases,^[4] has attracted extensive attention of chemists due to its advantages of high selectivity, mild reaction conditions, and environmental friendliness.^[5] The ω -transaminases are capable of catalyzing the asymmetric amination from prochiral ketones to chiral amines with strict stereoselectivity and 100% theoretical yield,^[6] indicating that they are promising biocatalysts for the production of chiral amines. However, due to the low solubility of organic substrates in the aqueous phase, it is difficult for enzyme to convert substrates towards the desired product.

Biocatalysis in organic solvents is high-efficient for converting organic substrates. Organic solvents can dissolve more nonpolar substrates^[7] and restrain microbial growth and pollution.^[8] Biocatalysis in organic phase is helpful for the separation and purification of products due to the low boiling points of organic solvents.^[9] Benefiting from these advantages, biocatalysis in organic solvents has been employed to produce

various high value-added products.^[10] However, the stability of enzymes is poor, and the activity is decreased or even inactivated in high concentration organic solvents. Therefore, improving the enzyme resistance and clarifying the mechanism of enzyme stability in organic solvents are needed.^[7]

The method for improving the stability of enzymes in organic solvents can be achieved by rational (semi-rational) design and random mutation.^[11,12] Tian et al. reported a semi-rational method for improving methanol tolerance of *Thermomyces lanuginosus* lipase,^[13] which aimed for the high B-factor residues^[14] to perform iterative saturation mutagenesis (ISM). In the directed evolution campaign of metalloprotease PT121 via random mutation, eleven variants with enhanced stability against 25% (*v/v*) acetonitrile were obtained.^[15] The beneficial “wing-type gate” for improving organic solvents resistance of ω -ATA from *Arthrobacter cummingsii* ZJUT212 was identified via a semi-rational design and two beneficial variants were obtained.^[16] Strengthening protein surface hydration via surface charge engineering combined with molecular dynamics (MD) simulation is an efficient rational strategy for tailoring enzyme stability in organic solvents.^[17] Meng et al. obtained two optimal ω -transaminase mutants from *Pseudomonas jessenii* with improved activity and high concentrations of isopropylamine and co-solvent tolerance by computational interface design.^[18] Generally, the design principle is still a considerable challenge for constructing a “small and smart” mutation library. Combining the advantages of rational design and random mutation will be helpful in obtaining more positive mutants quickly and efficiently.^[19,20]

In our previous work, wild type (WT) of amine transaminase from *Aspergillus terreus* (*At* ATA) has been cloned and expressed in *Escherichia coli*, and *At* ATA showed excellent catalytic efficiency and high *R*-enantioselectivity toward various ketones.^[21,22] Herein, the substrate 1-acetylnaphthalene could be catalyzed to produce (*R*)-NEA by *At* ATA. However, engineering of *At* ATA to develop a robust biocatalyst for green biomanufacturing of (*R*)-NEA is in huge demand due to the poor stability in organic solvents. In this study, we identified the critical hot spots by a strategy of regional random mutation, which analyzed the structure of *At* ATA, performed the error-prone PCR (epPCR) and combinatorial mutation, to evolve the organic solvents resistance of *At* ATA. For the “best” variant, its enzymatic properties towards 1-acetylnaphthalene in different organic solvents were performed in detail. Moreover, the underlying molecular mechanism was clarified by docking analysis and MD simulations.

2 Materials and methods

2.1 Materials

E. coli BL21(DE3) used for cloning and recombinant protein expression was purchased from TransGen Biotech Co. Ltd. (Beijing, China). The strain *E. coli* BL21(DE3)/pET28a(+)-*At* ATA was constructed in previous work and preserved in our laboratory.^[22] Prime STAR[®] Max DNA polymerase was purchased from Takara Biotechnology (Dalian, China). The restriction enzyme *Dpn* I was purchased from Thermo Scientific (Shanghai, China). All polymerase chain reaction (PCR) primers were synthesized by Tsingke Biological Technology (Hangzhou, China) and listed in Table S1. Other chemicals were of analytical grade and obtained from standard commercial sources.

2.2 Methods

2.2.1 Selection of organic solvent

According to the log *P* values, seven organic solvents containing acetonitrile (ACN), acetone (AC), methanol (MeOH), dimethyl sulfoxide (DMSO), *N,N*-dimethylformamide (DMF), isopropanol (IPA), and ethanol (EtOH) were selected for co-solvent of *At* ATA in this study. The reaction mixture contained 1-(*R*)-phenylethylamine (1-(*R*)-PEA) (5 mM), 1-acetylnaphthalene (5 mM), PLP (0.1 mM), the purified enzyme of *At* ATA-WT, and different organic solvents (the concentration ranging from 5~50%, *v/v*). The reactions were performed at 30 °C, 500 rpm for 30 minutes and the product (*R*)-NEA was analyzed by high performance liquid chromatography (HPLC). One unit of enzyme activity (U) was defined as the amount of enzyme required for 1 μ mol of (*R*)-NEA formed per minute under optimum conditions. The specific activity was expressed as the units of activity per gram purified enzyme (U/g). All experiments were conducted in

triplicates.

2.2.2 Mutagenesis and screening

Three regions of amino acid sequence fragments were selected to construct mutagenesis libraries via *in situ* epPCR based on WT as template. MnCl_2 (0.1 mM) was added to the PCR mixture to control the mutagenesis rate (1 to 2 mutation sites per gene). The PCR product was digested by *Eco* R I and *Xho* I, and ligated to the vector pET-28a. The PCR reaction conditions were supplemented in Table S2 to Table S5, and the template was digested by *Dpn* I at 37 °C for 0.5 h (refer to Table S6 for details). The PCR products were transformed into *E. coli* BL21 (DE3) competent cells for enzyme expression.

Colonies were picked up in 96 deep-well plates containing 1 mL of LB medium with 50 $\mu\text{g}/\text{mL}$ kanamycin and cultured for 8 h at 37 °C. Subsequently, isopropyl β -D-1-thiogalactopyranoside (IPTG) was added to 96 deep-well plates with a final concentration of 0.1 mM to induce protein expression. After incubation for 20 h at 25°C, the cells were harvested by centrifugation for 15 min at 3900 \times g. The cells in 96 deep-well plates were resuspended in 250 μL PBS buffer (100 mM, pH 8.0) with 5 mg/mL lysozyme at 37 °C for 30 min. The crude enzyme solution was centrifuged for 30 min at 3500 \times g. Next, 50 μL crude enzyme solution and 50 μL of 80% (*v/v*) DMSO was added to a new 96-well plate and incubated at 30 °C for 30 min.

A chromogenic reaction-based screening method was developed. In this section, 10 mM 1-(*R*)-PEA, 40% (*v/v*) DMSO, 25 mM 4-nitrophenylethylamine, 50 mM sodium phosphate (pH 8.0), 0.1 mM PLP, and enzymes incubating by 40% (*v/v*) DMSO, were added to 96-well plate at 30 °C, 600 rpm for 30 min.^[23] The absorbance values of the reaction solution were measured in 96-well microtiter plates at 500 nm using SpectraMax 190 Microplate Reader (Molecular Devices, USA), and Optical Density at 500 nm (OD_{500}) was calculated.

2.2.3 Protein expression and purification

All enzymes that we constructed were expressed and purified as described in our previous work.^[24] The mutants and WT with His₆-Tag were purified by nickel affinity chromatography and analyzed by SDS-PAGE.

2.2.4 Determination of kinetic parameters and half-lives in different concentration DMSO

The purified *At* ATAs were incubated in different concentrations of DMSO (the concentration ranging from 15~45%,*v/v*) for 15 min, and the temperature was maintained at 30 degC. Then, enzyme activity assay was performed. Each sample of 1 mL mixture was centrifuged at 13800 xg for 2 min, and the supernatant was subjected to microfiltration with 0.22 μm PTFE organic membranes. The product and remaining substrate were analyzed by HPLC to measure the 1-acetylnaphthalene conversion, (*R*)-NEA yield, and enantiomeric excess (*e.e.*). All the assays were conducted in triplicate.

The half-lives ($t_{1/2}$) of *At* ATAs were determined by incubating each purified enzyme (1 mg/mL) for appropriate times in different concentrations of DMSO (25%, 35%, and 45%,*v/v*) at 30 °C, respectively, followed by measuring the residual activity. The half-lives were calculated according to the first order deactivation equation 1 and 2:

$$\ln(A/A_0) = -k_d t \text{ (equation 1)}$$

$$t_{1/2} = \ln 2 / k_d \text{ (equation 2)}$$

where A_0 is the initial activity, A is the residual activity at time t during the thermal deactivation, k_d is the deactivation rate constant (min^{-1})

2.2.5 Enzyme kinetics characterization under different concentrations of DMSO

The reaction solution was added to DMSO (the final concentration of DMSO to 25%, 35%, or 45%, *v/v*). The initial rates were measured at various concentrations of 1-acetylnaphthalene in a range of from 0.1 to 15 mM with a fixed 1-(*R*)-PEA concentration (5 mM) and PLP (0.1 mM). For 1-(*R*)-PEA, 1-acetylnaphthalene

(5 mM) and 1-(*R*)-PEA in the range of 0.1 to 1.5 mM were used for the enzyme kinetic assays. The kinetic parameters were obtained by nonlinear fitting the experimental data to Michaelis-Menten equation.^[25,26]

2.2.6 MD simulation

The starting model was generated from the crystallography structure (PDB ID: 4CE5).^[22] The models of the variants were generated by FoldX software. MD simulations of *At* ATAs were performed via software YASARA at 308 K for 20 ns under AMBER14 force field.^[24] A cubic box was constructed that filled with 15~45% (*v/v*) DMSO. The simulation system was constructed with 15818~36056 water molecules, the number of which varied depending on the DMSO concentration. Counterions Na⁺ and Cl⁻ were used to neutralize the total net charge of the systems, and all resulting systems had a net charge of zero. During the simulation, coordinates, energies, and velocities were stored per 0.5 ns for further analysis.

2.2.7 Asymmetric synthesis of (*R*)-NEA by WT and mutant M3

The bio-asymmetric ammoniation 1-acetylnaphthalene to produce (*R*)-NEA was performed in a 20-mL scale reaction including 6.0 g_{dry cell weight}/L recombinant *E.coli* whole cells expressing WT or M3, 3~20 mM 1-(*R*)-PEA, 3~20 mM 1-acetylnaphthalene, and 25% (*v/v*) DMSO at 30 degC, 600 rpm. The yield and *e.e.* value of (*R*)-NEA were assayed via HPLC.

2.2.8 Analytical methods

The *e.e.* value of the product was determined after derivatization with Marfey's reagent (1-fluoro-2,4-dinitrophenyl-5-L-alaninamide, FDAA) as follows: 50 μ L of the reaction solution was mixed with 100 μ L of 1% (*m/v*) FDAA solution in acetone and 20 μ L of NaHCO₃ solution. After incubation at 40 °C for 2 h, 20 μ L of 2 M HCl was added to terminate the reaction. The samples were extracted with 3 times volume of dichloromethane, and evaporated at room temperature. Then, samples were dissolved in 50% (*v/v*) acetonitrile aqueous solution for HPLC analysis. An HPLC 1220 Infinity II system (Agilent Technologies) with an EC-C18 column (4.6 \times 150 mm, 4 μ m) was used at 30 °C. Detector wavelength was set at 340 nm. The mobile phase was composed of acetonitrile and ultra-pure water at a volumetric ratio of 60: 40 (*v/v*), and ran at a flow rate of 1 mL/min for 8 min.

The contents of 1-acetylnaphthalene and (*R*)-NEA were quantitatively analyzed by using an HPLC 1220 Infinity II system (Agilent Technologies) with a C-18 column (4.6 \times 150 mm, 4 μ m). Detector wavelength was set at 210 nm. The mobile phase was composed of 0.15% ethanolamine, acetonitrile and ultra-pure water at a volumetric ratio of 1 : 39 : 60 (*v/v/v*), and ran at a flow rate of 1.0 mL/min. The column temperature was maintained at 30 °C. Each measurement was conducted at least 3 times with a standard deviation of less than 5%.

3. Results and discussion

3.1 Determination of enzyme activity under different organic solvents

ACN, AC, MeOH, DMSO, DMF, IPA, and EtOH are the representatively and commonly used organic solvents with different log P values. The enzyme activities of *At* ATA in different concentrations of organic solvents were shown in Figure 1. All seven kinds of organic solvents had good solubility for 1-acetylnaphthalene (5 mM), and the activity of *At* ATA in DMSO was higher than other six organic solvents. Enzyme in 25% (*v/v*) DMSO displayed the highest activity, which the specific activity reached 8.86 U/g and the activity showed a bell-shape trend with the DMSO concentration increasing. Instead, the enzyme activities were decreased when the concentrations of other six organic solvents increased. Many reports indicated that DMSO was extensively used in the fields of organic synthesis and biocatalysis due to its favorable properties (amphiphilicity, dissolving ability, low chemical reactivity).^[27,28] In the following experiments, DMSO was selected as the organic solvent in this study.

Figure 1

3.2 Identification of *At* ATA key amino acid sites for improving organic solvents stability via regional epPCR

The crystal structure of *At* ATA-WT has been reported (PDB ID: 4CE5) and it is a homodimer with a substrate-binding pocket located in the dimer interface.^[22] In each monomer, there are three main loop regions on the surface and one of the three loop regions is located at the homodimer interface. Many literatures suggest that multimer interfaces of enzymes are essential for their stability since the interfaces are more hydrophobic and form a number of inter-H-bonds and hydrophobic interactions between subunits for affecting the overall function of protein.^[29] Besides, loop regions in the surface-exposed position of enzyme represent a potential targeting hot location for improving organic solvents tolerance, since enzyme requires some essential water to bound to the surface of enzyme for exhibiting conformational flexibility and maintaining the enzyme structure intact via H-bonds.^[28,30] Subsequently, regional epPCR covering amino acid residues at the three main loop regions was designed and conducted (Figure 2). The residue methionine (Met) at position 1 is not considered since it is translated from the initiation codon. Three epPCR libraries were generated by adding 0.1 mM MnCl₂ on the regional *At* ATA gene (from the 2nd to 30th containing a segment of α -helix, 75th to 105th, 197th to 261st bp) using *At* ATA-WT as template. High-throughput screening was performed using 4-nitrophenylethylamine and 1-acetylnaphthalene as substrates. As shown in Figure 3, about 9600 clones (96-well per plate \times 100 plates) were constructed to assay the residual activity, which 95.8% (9196 clones) lost or not detected their activity, and 404 clones remained activity. Notably, four mutants containing A13V/T200K, L91P/T200K, T23I, and P260S exhibited improved residual activity against high concentration DMSO (incubated in 80% DMSO, *v/v*), which were 60.7%, 59.2%, 55.3%, and 64.5% higher than WT, respectively. Furthermore, the mutants obtained from epPCR were re-screened at the optimal DMSO concentration (25% DMSO, *v/v*, Figure 3B), all four mutants were acquired with enhanced activity and stability against DMSO, and the single mutant T23I obtained the highest activity enhancement. Four mutants contained 5 amino acid residues (A13, T200, L91, P260, and T23). Combinatorial mutations were performed to obtain a “best” mutant against high concentration DMSO. As shown in Figure 4, the residual activities of single-, double- and triple-mutant incubated in different concentrations of DMSO were assayed. With the DMSO concentration increasing, the residual activity of WT and mutants decreased gradually. Compared with WT, double-mutant T200K/P260S and triple-mutant L91P/T200K/P260S, T23I/T200K/P260S displayed higher activities under different DMSO concentrations. And under 15~45% DMSO concentration, the “best” triple-mutant T23I/T200K/P260S exhibited the highest activity against DMSO. T23I/T200K/P260S was set as the research object in the following work.

Figure 2

Figure 3

Figure 4

3.3 Determination of organic solvent resistance against different DMSO concentrations

The organic solvent resistance of WT and the “best” mutant M3 against different DMSO concentrations was performed. The purified enzymes of WT and M3 were incubated in 25%, 35%, and 45% DMSO. The samples were incubated for 1~500 min and collected for activity measurement. Under 25% DMSO, the half-life ($t_{1/2}$) of M3 was 114.4 min, which was 61.6 min longer than WT (52.8 min). As the DMSO concentration increased to 35% and 45%, the $t_{1/2}$ of WT decreased to 48.7 and 13.5 min, respectively, whereas M3 was decreased to 75.6 and 19.4 min, respectively (Table 1). The $t_{1/2}$ values of WT and M3 suggested that the substitutions of T23I, T200K, and P260S were beneficial for *At* ATA overall structure against DMSO concentration. The specific activities of M3 in 25%, 35%, and 45% of DMSO were higher than WT. The phenomenon of activity-stability trade-off was off-target, whereas variant M3 displayed co-evolution toward activity and DMSO tolerance. In general, the residues affecting stability often appear in the loop of protein surface, and the residues affecting activity are often located near the active center. However, in many other cases of trade-off escape between activity and stability, the location of beneficial substitution is far from enzyme active site.^[31-33] The beneficial residue position 23, 200, and 260 in *At* ATA with improving the organic solvents stability, locate at loop region of surface that are far from active center, which may explain why M3 enhanced organic solvent stability without sacrificing activity.

Table 13.4 Determination of *At* ATAs' kinetic parameters under different DMSO concentrations

To investigate the catalytic efficiency of T23I/T200K/P260S, the kinetic parameters were assayed by using 1-acetylnaphthalene (amino acceptor) and 1-(*R*)-PEA (amino donor) as substrates. Under 25%, 35% and 45% DMSO, M3 displayed higher k_{cat} values than WT toward 1-acetylnaphthalene. And the K_{m} values of M3 for 1-acetylnaphthalene decreased compared with WT under different concentrations of DMSO (13.44, 14.70, and 30.27 mM *vs* 15.84, 22.01, and 43.62 mM, Table 2). The catalytic efficiency ($k_{\text{cat}}/K_{\text{m}}$) between WT and M3 had little difference. As for 1-(*R*)-PEA, the two enzymes of WT and M3 showed similar k_{cat} values. However, the K_{m} values of M3 decreased significantly. The $k_{\text{cat}}/K_{\text{m}}$ values of M3 increased 7.25-, 5.66-, and 3.67-fold higher than WT under 25%, 35%, and 45% DMSO toward 1-(*R*)-PEA. With the DMSO concentration increasing, the catalytic efficiency of WT and M3 gradually reduced, which indicated that the high concentration of DMSO could inhibit the catalytic efficiency or destroy the optimal conformation of *At* ATA toward 1-acetylnaphthalene and 1-(*R*)-PEA.

Table 2

3.5 Organic solvents resistance of WT and M3

In order to verify the resistance of M3 and WT against other organic solvents with different log P, $t_{1/2}$ values were assayed under 25% concentration of MeOH, ACN, DMF, EtOH, IPA, and AC. As shown in Table 3, the $t_{1/2}$ values of M3 were longer than WT under all six organic solvents. However, the $t_{1/2}$ values of M3 were different in various organic solvents, and the resistance of M3 against MeOH and DMF was stronger than against ACN, EtOH, IPA, and AC. This was related to the properties of different organic solvents, such as polarity, permittivity, viscosity, etc.^[34] Overall, M3 enhanced the stability against various organic solvents compared with WT significantly.

Table 3

3.6 MD simulations of WT and M3

For investigating the structural stability of the “best” mutant M3 with improved organic solvents stability, MD simulations of WT and M3 were performed at 308 K for 20 ns. The parameter of Root-mean-square deviation (RMSD) is used for exploring the fluctuation of protein conformation, and protein stability is negatively correlated with its RMSD values.^[35] As shown in Figure 5A, C, E, and G, M3 reached its equilibrium earlier than WT under different concentrations of DMSO, and the overall RMSD values of WT were higher than M3. The average RMSD values for WT were 1.733, 1.917, 1.922, and 1.981 Å, whereas the values for M3 declined to 1.521, 1.557, 1.598, and 1.603 Å. These results indicated that mutant M3 was more rigid than the WT under different concentrations of DMSO (ranging from 15%~45%, *v/v*) at 308 K. The results of Root-mean-square fluctuations (RMSF) were presented in Figure 5B, D, F, and H, representing the degree of freedom of each atom in a protein, and the residues with larger RMSF values reflected more degrees of freedom than those with smaller RMSF values.^[35] The overall RMSF plots of WT at different concentrations of DMSO were matched with M3. However, the regions of the mutation sites had apparent changes. The RMSF values of the N-terminal loop and C-terminal loop were decreased from WT to M3. The residues 23~30, 198~200, and 258~260 in WT had higher RMSF values than M3 (Table S8). And the average RMSF values of the overall structures decreased from 1.147, 1.180, 1.063, and 1.021 Å on WT to 1.121, 1.097, 0.972, and 0.982 Å on M3 under 15%, 25%, 35% and 45% DMSO, respectively. The reduction of regional and global amino acid RMSF values indicated that the mutant M3 had lower flexibility, which would significantly contribute to its organic solvent stability in different concentrations of DMSO.

Figure 5

3.7 Clarifying the mechanism of organic solvents stability enhancement

In order to investigate the effect of solvent on enzyme surface, the parameter of Solvent Accessible Surface Area (SASA) was calculated via Discovery Studio Client 2019. SASA is the surface area of biomolecules that

can be contacted by solvent, and a SASA value represents the aggregation-related properties of enzymes. A smaller SASA value implies a tighter packed structure of enzymes.^[34] As shown in Figure 6, the average SASA value of WT was 22244.4 Å², and, the value of M3 reduced to 22163.2 Å². The decreased SASA value of M3 suggested that the combinatorial mutation of triple mutants resulted in a more tightly packed structure to enhance the organic solvents stability.

Figure 6

The interactions within or between molecules are the main structural factors for stabilizing the overall or local structures, especially hydrogen bonds and hydrophobic interactions. Pace et al. reported that hydrophobic interactions and hydrogen bonds contribute approximately $60 \pm 4\%$ and $40 \pm 4\%$ to protein stability, respectively.^[36] As shown in Figure 7, the interactions of mutation sites with surrounding amino acids were displayed. When Thr200 was substituted with Lys200, additional H-bonds (between site 200 and Ser160) and hydrophobic interaction (between site 200 and Met154) were increased. When Pro260 was mutated to Ser, a H-bonds was added between Ser260 and Leu263, and the distance of hydrophobic interaction between site 260 and Leu263 decreased from 5.495 Å to 5.221 Å. As for site 23, there was no increase or decrease of H-bond and hydrophobic interaction. The substrate binding pocket locates on the dimer interface of *At* ATA, and the substitution of local amino acids will influence the interaction between or within monomers so that the overall structure conformation may change. Via Discovery Studio 2019 Client, the number of H-bond, electrostatic, hydrophobic, and salt bridge between or within molecules of WT or M3 was counted (Table 4). The total number of interactions between or within monomers was increased from WT to M3. This might strengthen the rigidity of mutant structure for resisting the organic solvents. For dimer or multimer proteins, the subunit interface is crucial for stability, and the protein structure can be optimized by stabilizing the subunit interface. As shown in Figure 8, the hydrophobic interactions and H-bonds on the dimer interface of WT and M3 were further analyzed using the software Ligplus, and the H-bonds and hydrophobic interactions were increased from WT to M3, which could improve the rigidity of the interface, so that promote a more compact joint between two monomers. In general, the enhanced rigidity may lead to a slight decrease in catalytic efficiency.^[37] In this study, the catalytic efficiency of M3 was not decreased, which might be these three sites were far from the active site K180, and they were not cause significant changes to the substrate binding pocket.

Figure 7

Figure 8

In addition to the increase of interactions within or between proteins for improving the stability of proteins, the interaction between solvent molecules and proteins in the reaction system is also a key factor. Organic solvents can interact with residues on the surface of enzyme and affect the structure of the enzyme.^[8,28] Water molecules attached to the enzyme surface would make the enzyme and the substrate bind better, and maintain enzyme activity and stability via noncovalent interactions.^[9,34] Organic solvent will compete with water molecules for enzymes, reducing the surface water layer of enzyme, thereby changing the structure of the protein and changing its stability.^[9,38,39] Herein, three mutation sites T23, T200, and P260 obtained by regional epPCR were located in the loop on the surface of the *At* ATA. The mutated amino acids K200 and S260 are polar amino acids, respectively, and their residues are more easily combined with water molecules to increase the hydration shell on the protein surface and maintain enzyme activity and organic solvent resistance. However, site 23 of polar amino acid threonine on WT was substituted with nonpolar amino acid isoleucine, and the organic solvents stability was not decreased. This might be site 23 is located at the N-terminal of *At* ATA, the hydrophobic side chains prefer to be buried within the core of the protein rather than been exposed to organic solvents to make the overall structure in a more favorable state.^[40]

3.8 Asymmetric synthesis of (*R*)-(+)-1-(1-naphthyl) ethylamine by recombinant *E. coli* whole cells expressing WT and M3

Compared with purified enzyme, whole cells as bio-catalyst can reduce the time and cost of purification, simplify the cofactor regeneration system and require no additional expensive external cofactors.^[41] Fur-

thermore, whole cells can protect and stabilize the enzymes for resisting severe external environments.^[42] Moreover, whole cells as bio-catalyst can simplify the separation and purification of downstream processing for acquiring target products.^[43] In order to optimize the amplification experiment using whole cells, the substrate concentration was set as 3~20 mM in 20-mL scale. The substrates of 3~20 mM 1-acetylnaphthalene and 1-(*R*)-PEA were dissolved in 25% DMSO due to the activity of *At* ATA in 25% DMSO was considerably higher than that in higher concentration DMSO, and the time course of the asymmetric synthesis of (*R*)-NEA in the presence of 25% DMSO was monitored and compared using 6 g dcw/L recombinant *E. coli* expressing WT and M3. As shown in Figure 9A, the substrate concentration was 3 mM, the yield of (*R*)-NEA using WT reached the maximum value of 88.3% within 5 h, while the yield of (*R*)-NEA using M3 reached the maximum yield of 94.2% after 7 h. With the substrate concentration increased to 5, 10, 15, and 20 mM, the yield of (*R*)-NEA catalyzed by M3 was higher than that of WT, and the yield catalyzed by both WT and M3 was decreased. All the reactions reached equilibrium within 10 h and the optical purity of (*R*)-NEA was > 99.5% (Table 5). Overall, improving the tolerance of organic solvents for M3 plays a vital role in asymmetric synthesis (*R*)-NEA.

Figure 9

4 Conclusions

In summary, biocatalysis in organic solvents is very appealing for the industry in producing many intermediates and fine chemicals, and improving the organic solvents stability of enzyme is urgent for biomanufacturing via protein engineering. The beneficial mutation sites were identified via regional random mutation, and the best mutant T23I/T200K/P260S (M3) was obtained by combinatorial mutation, which not only enhanced the resistance against organic solvents, but also improved the catalytic efficiency of the enzyme. MD results showed that increasing the rigidity of the loop region on the protein surface displayed a positive correlation with organic solvents resistance. And the increase of intra- and intermolecular interactions stabilized the protein structure so that mutant could tolerate high concentration organic solvents. Under 25% DMSO, M3 displayed better catalytic performance toward 1-acetylnaphthalene than WT. In conclusion, M3 is a potential excellent biocatalyst for the synthesis of (*R*)-NEA due to its high organic solvent stability.

Authors' contributions The design and conduct of experiments were executed by J. Huang, S. Qiu, C. N. Wang, C. J. Lyu, F. F. Fan, S. Hu and W. R. Zhao. The writing and revising of manuscript were done by S. Qiu, J. Q. Mei, and C. N. Wang. Project administration was in the charge of J. Huang and L. H. Mei. All authors read and approved the manuscript

Funding This research was funded by the National Natural Science Foundation of China (Nos. 32071268, 32201037, 31971372, 22103071), Ningbo “Scientific and Technological Innovation 2025” Key Project (2020Z080).

Data availability All data and materials are available upon reasonable request.

Declarations

Conflict of interest The authors declare that they have no conflict of interest.

Ethical approval This article does not contain any studies with human participants or animals performed by any of the authors.

Reference

- Blaser, H. U. (2003). Enantioselective catalysis in fine chemicals production. *Chemical Communications* , 3 , 293-296.
- Dudas, J., & Hanika, J. (2009). Design, scale up and safe piloting of thymol hydrogenation and menthol racemization. *Chemical Engineering Research & Design* , 87 , 83-90.
- Thiel, O. R., Bernard, C., Tormos, W., Brewin, A., Hirotsu, S., Murakami, K., Saito, K., Larsen, R. D., Martinelli, M. J., & Reider, P. J. (2008). Practical synthesis of the calcimimetic agent, cinacalcet. *Tetrahedron Letters* , 49 , 13-15.

4. Truppo, M. D., Turner, N. J., & Rozzell, J. D. (2009). Efficient kinetic resolution of racemic amines using a transaminase in combination with an amino acid oxidase. *Chemical Communications*, *16*, 2127-2129.
5. Bilal, M., & Iqbal, H. M. N. (2019). Tailoring multipurpose biocatalysts via protein engineering approaches: A review. *Catalysis. Letters*, *149*, 2204-2217.
6. Kelly, S. A., Pohle, S., Wharry, S., Mix, S., Allen, C. C. R., Moody, T. S., & Gilmore, B. F. (2018). Application of ω -transaminases in the pharmaceutical industry. *Chemical Reviews*, *118*, 349-367.
7. Gupta, M. N., & Roy, I. (2004). Enzymes in organic media: Forms, functions and applications. *European Journal of Biochemistry*, *271*, 2575-2583.
8. Carrea, G., & Ho, W. S. (2000). Properties and synthetic applications of enzymes in organic solvents. *Angewandte Chemie International Edition*, *39*, 2226-2254.
9. Kumar, A., Dhar, K., Kanwar, S. S., & Arora, P. K. (2016). Lipase catalysis in organic solvents: Advantages and applications. *Biological Procedures Online*, *18*, 2.
10. Ogino, H., & Ishikawa, H. (2001). Enzymes which are stable in the presence of organic solvents. *Journal of Bioscience and Bioengineering*, *91*, 109-116.
11. Bornscheuer, U. T., Huisman, G. W., Kazlauskas, R. J., Lutz, S., Moore, J. C., & Robins, K. (2012). Engineering the third wave of biocatalysis. *Nature*, *485*, 185-194.
12. Stepankova, V., Bidmanova, S., Koudelakova, T., Prokop, Z., Chaloupkova, R., & Damborsky, J. (2013). Strategies for stabilization of enzymes in organic solvents. *ACS Catalysis*, *3*, 2823-2836.
13. Tian, K., Tai, K., Chua, B. J. W., & Li, Z. (2017). Directed evolution of *Thermomyces lanuginosus* lipase to enhance methanol tolerance for efficient production of biodiesel from waste grease. *Bioresource Technology*, *245*, 1491-1497.
14. Reetz, M. T., & Carballeira, J. D. (2007). Iterative saturation mutagenesis (ISM) for rapid directed evolution of functional enzymes. *Nature Protocols*, *2*, 891-903.
15. Zhu, F., He, B., Gu, F., Deng, H., Chen, C., Wang, W., & Chen, N. (2020). Improvement in organic solvent resistance and activity of metalloprotease by directed evolution. *Journal of Biotechnology*, *309*, 68-74.
16. Cheng, F., Li, M. Y., Wei, D. J., Zhang, X. J., Jia, D. X., Liu, Z. Q., & Zheng, Y. G. (2022). Enabling biocatalysis in high-concentration organic cosolvent by enzyme gate engineering. *Biotechnology and Bioengineering*, *119*, 845-856.
17. Cui, H., Vedder, M., Zhang, L., Jaeger, K. E., Schwaneberg, U., & Davari, M. D. (2022). Polar substitutions on the surface of a lipase substantially improve tolerance in organic solvents. *ChemSusChem*, *15*, e202102551.
18. Meng, Q., Capra, N., Palacio, C. M., Lanfranchi, E., Otzen, M., Schie, L. Z., Rozeboom, H. J., Thunnissen, A. W. H., Wijma, H. J., & Janssen, D. B. (2020). Robust ω -transaminases by computational stabilization of the subunit interface. *ACS Catalysis*, *10*, 2915-2928.
19. Cheng, F., Zhu, L., & Schwaneberg, U. (2015). Directed evolution 2.0: Improving and deciphering enzyme properties. *Chemical Communications*, *51*, 9760-9772.
20. Gargiulo, S., & Soumillon, P. (2021). Directed evolution for enzyme development in biocatalysis. *Current Opinion Chemical Biology*, *61*, 107-113.
21. Fesko, K., Steiner, K., Breinbauer, R., Schwab, H., Schürmann, M., & Strohmeier, G. A. (2013). Investigation of one-enzyme systems in the ω -transaminase-catalyzed synthesis of chiral amines. *Journal of Molecular Catalysis B-Enzymatic*, *96*, 103-110.
22. Lyskowski, A., Gruber, C., Steinkellner, G., Schürmann, M., Schwab, H., Gruber, K., & Steiner, K. (2014). Crystal structure of an (*R*)-selective ω -transaminase from *Aspergillus terreus*. *PLoS One*, *9*, e87350.
23. Baud, D., Ladkau, N., Moody, T. S., Ward, J. M., & Hailes, H. C. (2015). A rapid, sensitive colorimetric assay for the high-throughput screening of transaminases in liquid or solid-phase. *Chemical Communications*, *51*, 17225-17228.
24. Cao, J. R., Fan, F. F., Lyu, C. J., Wang, H. P., Li, Y., Hu, S., Zhao, W. R., Chen, H. B., Huang, J., & Mei, L. H. (2021). Improving the thermostability and activity of transaminase from *Aspergillus terreus*

- s by charge-charge interaction. *Frontiers in Chemistry* , *9* , 664156.
25. Garrido-del Solo, C., García-Cánovas, F., Havsteen, B. H., & Varón-Castellanos, R. (1993). Kinetic analysis of a Michaelis-Menten mechanism in which the enzyme is unstable. *Biochemical Journal* , *294* , 459-464.
 26. Choi, B., Rempala, G. A., & Kim, J. K. (2017). Beyond the Michaelis-Menten equation: Accurate and efficient estimation of enzyme kinetic parameters. *Scientific Reports* , *7* , 17018.
 27. Tsuzuki, W., Ue, A., & Kitamura, Y. (2001). Effect of dimethylsulfoxide on hydrolysis of lipase. *Bioscience, Biotechnology, and Biochemistry* , *65* , 2078-2082.
 28. Tsuzuki, W., Ue, A., & Nagao, A. (2003). Polar organic solvent added to an aqueous solution changes hydrolytic property of lipase. *Bioscience, Biotechnology, and Biochemistry* , *67* , 1660-1666.
 29. Larsen, T. A., Olson, A. J., & Goodsell, D. S. (1998). Morphology of protein-protein interfaces. *Structures* , *6* , 421-427.
 30. Bellissent-Funel, M. C., Hassanali, A., Havenith, M., Henchman, R., Pohl, P., Sterpone, F., van der Spoel, D., Xu, Y., & Garcia, A. E. (2016). Water determines the structure and dynamics of proteins. *Chemical Reviews* , *116* , 7673-7697.
 31. Li, S. F., Xie, J. Y., Qiu, S., Xu, S. Y., Cheng, F., Wang, Y. J., & Zheng, Y. G. (2021). Semirational engineering of an aldo-keto reductase *Km* AKR for overcoming trade-offs between catalytic activity and thermostability. *Biotechnology and Bioengineering* , *118* , 4441-4452.
 32. Tokuriki, N., Stricher, F., Serrano, L., & Tawfik, D. S. (2008). How protein stability and new functions trade off. *PLoS Computational Biology* , *4* , e1000002.
 33. Stimple, S. D., Smith, M. D., & Tessier, P. M. (2020). Directed evolution methods for overcoming trade-offs between protein activity and stability. *AIChE Journal* , *66* (3), e16814.
 34. Cui, H., Stadtmüller, T. H. J., Jiang, Q., Jaeger, K. E., Schwaneberg, U., & Davari, M. D. (2020). How to engineer organic solvent resistant enzymes: Insights from combined molecular dynamics and directed evolution study. *ChemCatChem* , *12* , 4073-4083.
- Liu, J., Wei, B., Che, C., Gong, Z., Jiang, Y., SI, M., Zhang, J., & Yang, G. (2019). Enhanced stability of manganese superoxide dismutase by amino acid replacement designed via molecular dynamics simulation. *International Journal of Biological Macromolecules* , *128* , 297-303.
1. Pace, C. N., Fu, H., Fryar, K. L., Landua, J., Trevino, S. R., Shirley, B. A., Hendricks, M. M., Iimura, S., Gajiwala, K., & Scholtz, J. M. (2011). Contribution of hydrophobic interactions to protein stability. *Journal of Molecular Biology* , *408* , 514-528.
 2. Siddiqui, K. S. (2017). Defying the activity-stability trade-off in enzymes: Taking advantage of entropy to enhance activity and thermostability. *Critical Reviews in Biotechnology* , *37* , 309-322.
 3. Cui, H., Zhang, L., Eltoukhy, L., Jiang, Q., Korkunç, S. K., Jaeger, K. E., Schwaneberg, U., & Davari, M. D. (2020). Enzyme hydration determines resistance in organic cosolvents. *ACS Catalysis* , *10* , 14847-14856.
 4. Cui, H., Jaeger, K. E., Davari, M. D., & Schwaneberg, U. (2021). CompassR yields highly organic-solvent-tolerant enzymes through recombination of compatible substitutions. *Molecular Human Reproduction* , *27* , 2789-2797.
 5. Richard, J. P., Amyes, T. L., Malabanan, M. M., Zhai, X., Kim, K. J., Reinhardt, C. J., Wierenga, R. K., Drake, E. J., & Gulick, A. M. (2016). Structure-function studies of hydrophobic residues that clamp a basic glutamate side chain during catalysis by triosephosphate isomerase. *Biochemistry* , *55* , 3036-3047.
 6. Schuurmann, J., Quehl, P., Festel, G., & Jose, J. (2014). Bacterial whole-cell biocatalysts by surface display of enzymes: Toward industrial application. *Applied Microbiology and Biotechnology* , *98* , 8031-8046.
 7. Carballeira, J. D., Quezada, M. A., Hoyos, P., Simeo, Y., Hernaiz, M. J., Alcantara, A. R., & Sinisterra, J. V. (2009). Microbial cells as catalysts for stereoselective redox reactions. *Biotechnology Advances* , *27* , 686-714.
 8. Lin, B., & Tao, Y. (2017). Whole-cell biocatalysts by design. *Microbial Cell Factories* , *16* , 106.

Table 1. The half-life ($t_{1/2}$) and specific activity of WT and M3 under different concentrations of DMSO

		25% DMSO	25% DMSO	25% DMSO		35% DMSO	35% DMSO	35% DMSO
Enzyme	$t_{1/2}$ (min)	$t_{1/2}$ (min)	k_d (min^{-1})	Specific activity (U/g)	$t_{1/2}$ (min)	k_d (min^{-1})	Specific activity	
WT	52.8 ± 0.8	52.8 ± 0.8	0.013	4.7 ± 0.2	48.7 ± 1.2	0.014	2.6 ± 0.1	
M3	114.4 ± 4.4	114.4 ± 4.4	0.006	6.6 ± 0.3	75.6 ± 3.0	0.009	4.7 ± 0.2	

Table 2. Kinetic parameters of WT and M3 toward 1-acetylnaphthalene (A) and 1-(*R*)-PEA (B) under different concentrations of DMSO

A

	25% DMSO	25% DMSO	25% DMSO		35% DMSO	35% DMSO	35% DMSO
Enzyme	k_{cat} (min^{-1})	K_m (mM)	k_{cat}/K_m ($\text{L}\cdot\text{min}^{-1}\cdot\text{mmol}^{-1}$)		k_{cat} (min^{-1})	K_m (mM)	k_{cat}/K_m ($\text{L}\cdot\text{min}^{-1}\cdot\text{mmol}^{-1}$)
WT	0.45 ± 0.05	15.84 ± 0.81	0.028		0.34 ± 0.05	22.01 ± 1.36	0.015
M3	0.62 ± 0.04	13.44 ± 0.32	0.046		0.44 ± 0.04	14.70 ± 0.22	0.029

B

	25% DMSO	25% DMSO	25% DMSO		35% DMSO	35% DMSO	35% DMSO
Enzyme	k_{cat} (min^{-1})	K_m (mM)	k_{cat}/K_m ($\text{L}\cdot\text{min}^{-1}\cdot\text{mmol}^{-1}$)		k_{cat} (min^{-1})	K_m (mM)	k_{cat}/K_m ($\text{L}\cdot\text{min}^{-1}\cdot\text{mmol}^{-1}$)
WT	0.31 ± 0.02	0.16 ± 0.04	1.94		0.11 ± 0.01	0.17 ± 0.03	0.65
M3	0.32 ± 0.01	0.02 ± 0.01	16.00		0.13 ± 0.01	0.03 ± 0.01	4.33

Table 3. The $t_{1/2}$ values of WT and M3 against different organic solvents

Enzyme	$t_{1/2}$ in 25% MeOH (min)	$t_{1/2}$ in 25% ACN (min)	$t_{1/2}$ in 25% DMF (min)	$t_{1/2}$ in 25% EtOH (min)	$t_{1/2}$ in 25% MeOH (min)
WT	13.3 ± 0.6	3.5 ± 0.5	12.3 ± 0.4	2.0 ± 0.05	1.5 ± 0.05
M3	26.5 ± 1.0	7.2 ± 0.6	19.3 ± 0.5	5.6 ± 0.11	4.9 ± 0.1

Table 4. The interactions between or within molecules of WT or M3. The number of interactions between or within molecules is calculated by the software of Discovery

Studio 2019 Client.

Interaction Type	WT	WT	M3	M3
	Interaction between molecules	Interaction within molecules	Interaction between molecules	Interaction within molecules
Hydrogen Bond	39	808	43	824
Electrostatic	7	340	8	356
Hydrophobic ^a	28	83	36	89
Salt Bridge	8	21	8	28

^a The interaction cut-off value is 5 Å.

Table 5. The comparison of catalytic parameters evaluation for WT and M3

Enzyme	The concentration of DMSO (<i>v/v</i> , %)	Substrate load (mM)	Reaction time (h)	Yield (%)	Optical purity (%)
WT	25	3	10	88.3 ± 3.1	> 99.5% <i>R</i>
	25	5	10	17.3 ± 1.0	> 99.5% <i>R</i>
	25	10	10	10.9 ± 0.3	> 99.5% <i>R</i>
	25	15	10	4.3 ± 0.7	> 99.5% <i>R</i>
	25	20	10	2.3 ± 0.1	> 99.5% <i>R</i>
M3	25	3	10	94.2 ± 4.2	> 99.5% <i>R</i>
	25	5	10	69.5 ± 0.9	> 99.5% <i>R</i>
	25	10	10	38.9 ± 1.2	> 99.5% <i>R</i>
	25	15	10	15.3 ± 0.8	> 99.5% <i>R</i>
	25	20	10	8.7 ± 0.3	> 99.5% <i>R</i>

Figure 1. The specific activity of *At* ATA-WT in different types and concentrations of organic solvents. The reaction conditions: 0.5 mg/mL purified enzyme, 5 mM 1-(*R*)-PEA, 5 mM 1-acetylnaphthalene, 0.1 mM PLP and 5~50% (*v/v*) organic solvent. The reaction mixtures were shaken at 30 °C for 30 min.

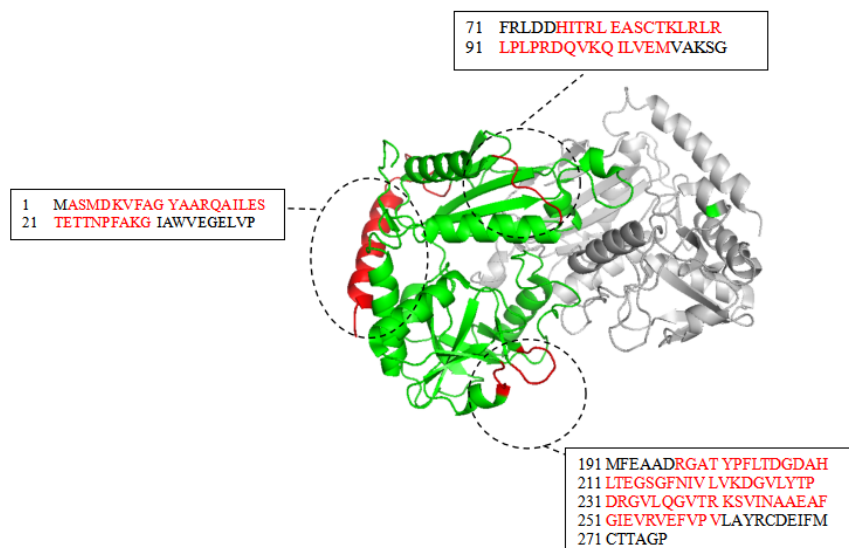


Figure 2. The structural model of *At* ATA (PDB ID: 4CE5) and the targeting regions for epPCR. The three loop regions and the corresponding sequences at the surface of enzyme were colored in red.

Figure 3. An overview of the effect of each mutant on *At* ATA-WT relative activity (A). All the mutants were incubated in 80% (*v/v*) DMSO for 30 min at 30 °C to assay the residual activity. The residual activity of *At* ATA-WT was defined as 100%. The specific activity of WT and mutants (B). The purified enzymes were incubated or no incubated in 25% DMSO for 15 min at 30°C to assay the specific activity.

Figure 4. Residual activities of WT and its variants toward 1-acetylnaphthalene. The purified enzymes were incubated in 15%, 25%, 35% and 45% DMSO for 15 min at 30°C. Then, the residual activity was assayed

in the mixtures containing 0.5 mg/mL purified enzymes, 5 mM 1-(*R*)-PEA ,5 mM 1-acetylnaphthalene, 0.1 mM PLP and 25% (*v/v*) DMSO at 30°C, 600 rpm for 30 min.

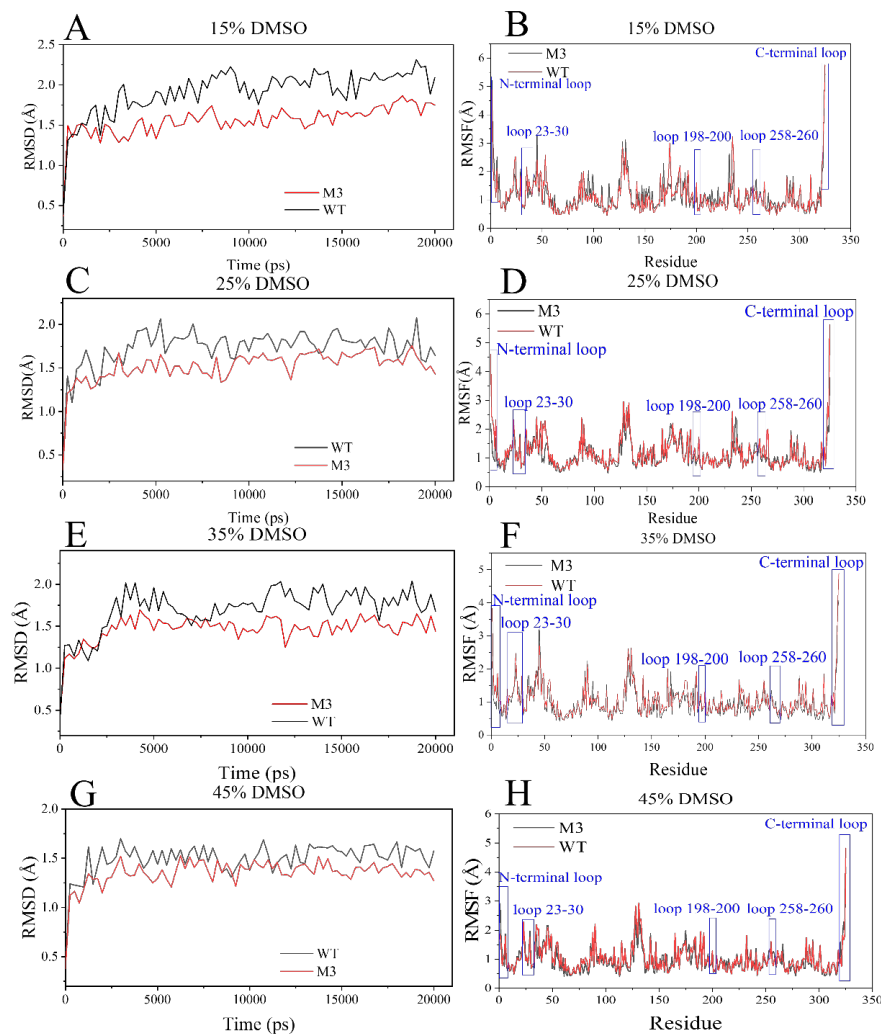


Figure 5. The RMSD and RMSF analysis of WT and M3. (A), (C), (E), and (G) were the RMSD analysis of WT and M3 under 15%, 25%, 35%, and 45% DMSO, respectively. (B), (D), (F), and (H) were the RMSF analysis of WT and M3 under 15%, 25%, 35%, and 45% DMSO, respectively. MD analysis was performed at 35°C during a 20-ns simulation.

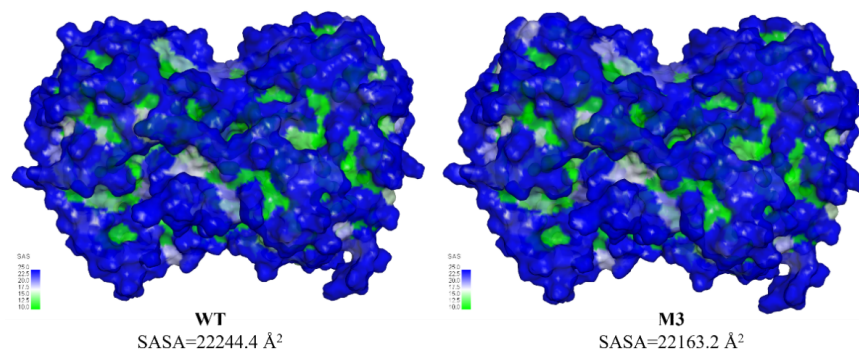


Figure 6. SASA values of WT and mutant M3. The surface models and SASA values were drawn and calculated by Discovery Studio Client 2019.

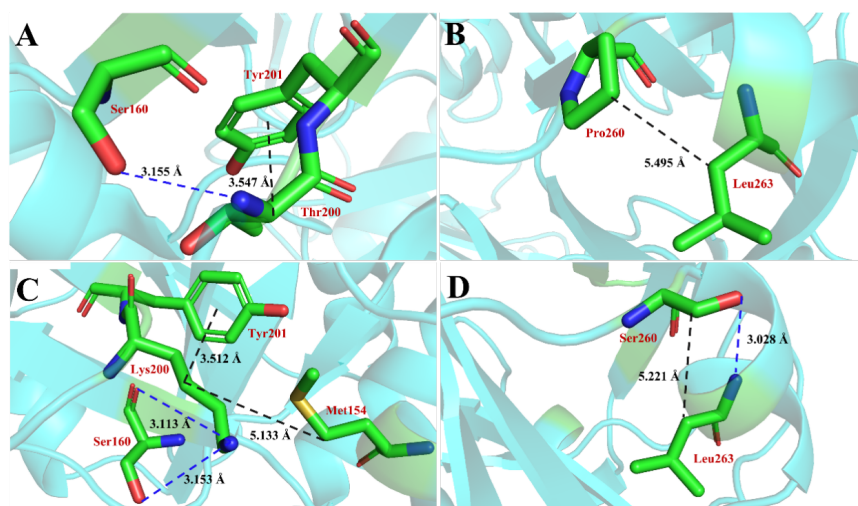


Figure 7. Interaction analysis between the mutation site and surrounding amino acids in WT and M3. (A and C are the interactions between the two original mutation sites and surrounding amino acids in WT; B and D are the interactions between the mutation sites and surrounding amino acids in M3. Blue dotted line represents hydrogen bond, black dotted line represents hydrophobic interaction).

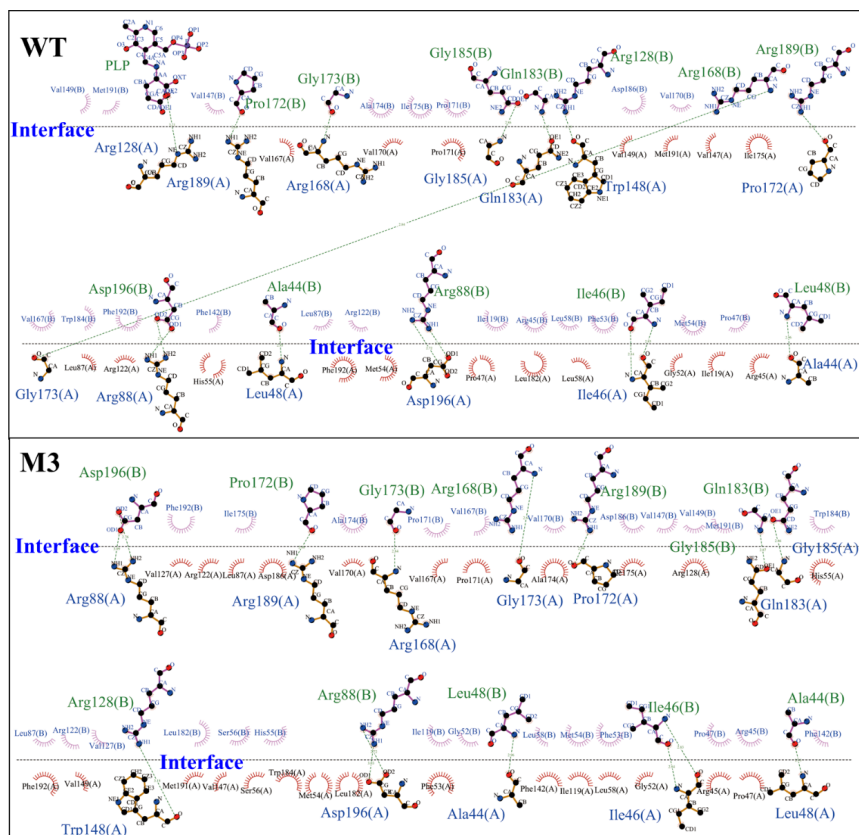


Figure 8. Interface hydrogen bonds and hydrophobic interactions analysis of WT and M3 using LigPlus. Green dashed lines represent hydrogen bonds; red diverging arcs represent hydrophobic interactions.

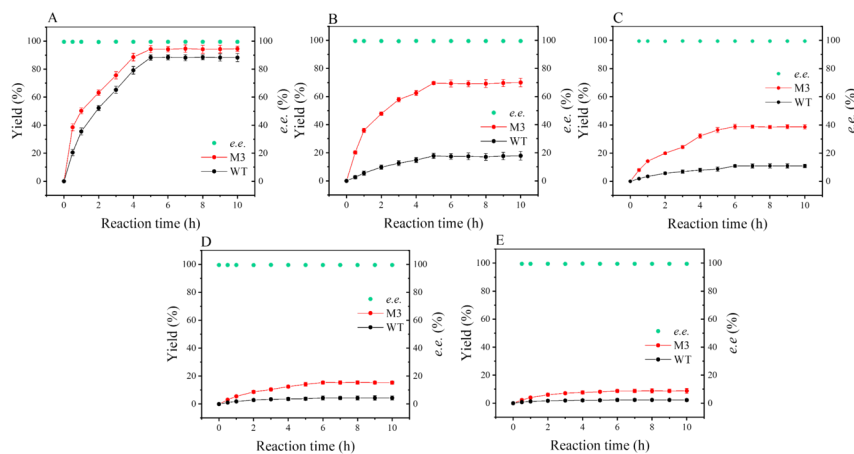
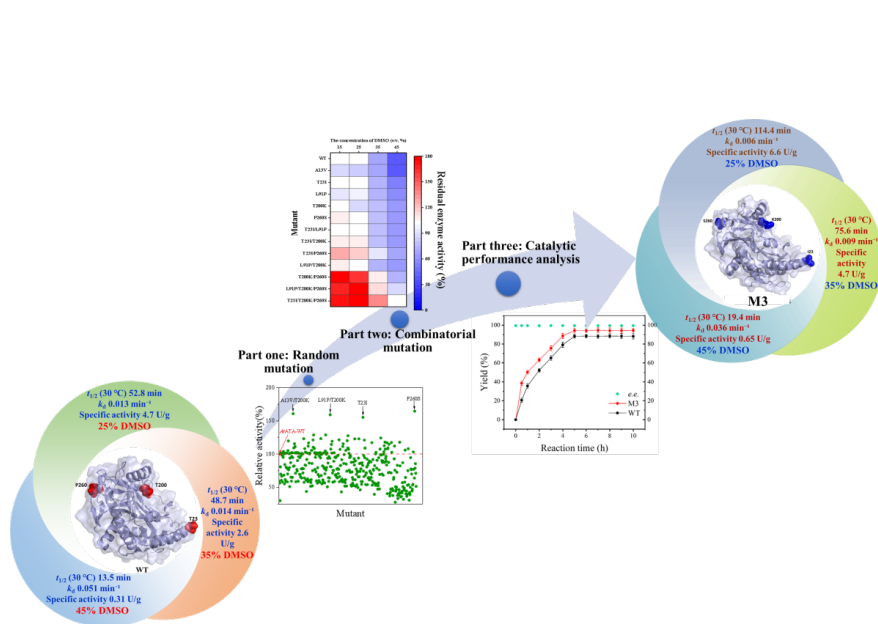


Figure 9. Time course of asymmetric synthesis of (*R*)-NEA on 20-mL scale by using recombinant *E. coli* whole cells expressing WT and M3. Reaction was performed with 3 mM (A), 5 mM (B), 10 mM (C), 15 mM (D), and 20 mM (E) 1-acetylnaphthalene and a corresponding equivalent 1-(*R*)-PEA in 50 mM, pH 8.0 PBS buffer with DMSO (25%, *v/v*) at 30°C.



Entry for the Table of Contents